J Mater Sci: Mater Electron (2009) 20:S159–S163
DOI 10.1007/s10854-007-9497-9

Silicon photonic waveguides for mid- and long-wave infrared region

Peng Yuan Yang · Stevan Stankovic · Jasna Crnjanski · Ee Jin Teo · David Thomson · Andrew A. Bettiol · Mark B. H. Breese · William Headley · Cristina Giusca · Graham T. Reed · Goran Z. Mashanovich

Received: 20 July 2007 / Accepted: 15 November 2007 / Published online: 4 December 2007

Abstract Silicon photonics is experiencing a dramatic increase in interest due to emerging application areas and several high profile successes in device and technology development (Liu et al Nature 427:615, 2004; Rong et al Nature 433:725, 2005; Almeida et al Nature 431:1081, 2004). Conventional waveguides in silicon photonics are designed for the telecom wavelengths. However, mid- and long-wave infrared regions are interesting for several application areas including sensing, communications, signal processing, missile detection and imaging (Soref et al J Opt A Pure Appl Opt 8:840, 2006). The most popular waveguide platform in silicon photonics is the Silicon-On-Insulator (SOI) structure, in the form of either a strip or a rib waveguide. This material structure, however, is not suitable for longer wavelengths (except in the 2.9–3.6 μm range) due to the absorption spectra of silicon dioxide (Soref et al J Opt A Pure Appl Opt 8:840, 2006). In this paper, we discuss the design and fabrication of two different waveguide structures, the freestanding (Yang et al Appl Phys Lett 90:241109, 2007) and hollow core waveguides (Stanković et al Proceedings of 51th Conference ETRAN, 2007). The former is suitable for long-wave infrared applications as it has an air cladding, whilst the latter is a candidate for sensing in the mid-wave infrared wavelength region.

P. Y. Yang (✉) · D. Thomson · W. Headley · C. Giusca · G. T. Reed · G. Z. Mashanovich
Advanced Technology Institute, University of Surrey, Surrey, UK
e-mail: p.yang@surrey.ac.uk

S. Stankovic · J. Crnjanski
Faculty of Electrical Engineering, University of Belgrade, Belgrade, Serbia

E. J. Teo · A. A. Bettiol · M. B. H. Breese
Department of Physics, National University of Singapore, Singapore, Singapore

1 Introduction

Mid-wave (MWIR) and long-wave infrared (LWIR) spectra are of interest in a variety of applications, such as sensing, imaging or medical applications. Research and design in silicon photonics has been primarily focused on devices optimised for 1.55 μm wavelength, utilised in telecommunications [1–3]. Relatively little attention was paid to silicon photonics waveguides optimised for larger wavelengths, though Soref et al. have recently proposed a number of waveguide structures suitable for MWIR and LWIR spectra [4]. In this paper, we discuss the design and fabrication of two candidate MWIR/LWIR waveguide structures, the freestanding and hollow core waveguides [5–10]. The former waveguide is fabricated by an advanced fabrication technique of proton beam writing (PBW). It has an air cladding, alternatively any other suitable cladding could be deposited to make the structures suitable for specific wavelength ranges. The latter candidate allows propagation of light in air, overcoming the fact that conventional waveguides, having a solid core suffer from several shortcomings related to the propagation of light through solid materials, such as dispersion and temperature dependence of the refractive index.

2 Fabrication of silicon freestanding waveguide by proton beam writing

PBW is a new direct-writing process that uses a focused beam of MeV or sub-MeV protons to pattern waveguide

components in silicon. The fabricating process is similar to e-beam writing, nevertheless it offers some interesting and unique advantages. Due to the large mass mismatch between protons and electrons ($m_p/m_e = 1800$), protons penetrate deeper into the semiconductor while maintaining a straight path. The trajectories of protons and electrons, can be simulated using the Monte Carlo technique such as used in SRIM [11] and Casino [12]. The calculation indicates that protons exhibit minimal proximity effects compared to electrons. This opens the way to allow PBW to be a direct-writing lithography technique in Si to produce high aspect ratio structures. Another unique characteristic of proton beams is that their penetration depth is well defined and can be controlled by changing the proton energy. This allows the fabrication of long distance freestanding structures. By employing this advantage, the world's first freestanding waveguide in Si have been realized by PBW and characterized in our previous work [5]. Finally, the irradiated dose is tunable in a pre-defined pattern, by pausing the proton beam for different amounts of time at selective locations. In this way, any pattern of localized damage can be built up. This feature can be used to produce three-dimensional multilevel structures in bulk p-type silicon [13]. Also this process enables local modifications and control of photoluminescence and electroluminescence properties of porous silicon, which offers the possibility of producing light emitting devices in Si substrate [14].

In this work, improved freestanding waveguide structures are fabricated by employing 0.5 MeV proton energy. The penetration range and energy deposition profile of 0.5 MeV protons are simulated by SRIM. A well focused proton beam of 200 nm resolution is used to irradiate the Si sample. The beam is magnetically scanned in the *x*-direction, which determines the width of the waveguide, in this case 5 μm wide, whilst simultaneously applying a constant linear perpendicular motion in the *y*-direction, provided by an Exfo Burleigh Inchworm stage. The proton fluence delivered to the sample is 5E14 proton/cm^2. After irradiation, the sample is electrochemically etched in a 1:1 electrolyte mixture of 48% HF and ethanol at a current density of 40 mA/cm^2. Once the silicon becomes porous, it can be removed by a dilute potassium hydroxide solution, producing a waveguide with an approximately square profile in the cross section. A scanning electron microscope (SEM) image of the waveguide cross section is shown in Fig. 1. The waveguide has a height of ~5.5 μm and width of ~5 μm at the top and ~6 μm at the bottom.

A source of propagation loss in freestanding waveguide is the intersection between the waveguide and the pillars. During work on the first freestanding waveguide chip, the thin silicon wires showed great mechanical strength. After dispensing a protective wax onto the chip for polishing, the waveguides bend significantly, however all waveguides

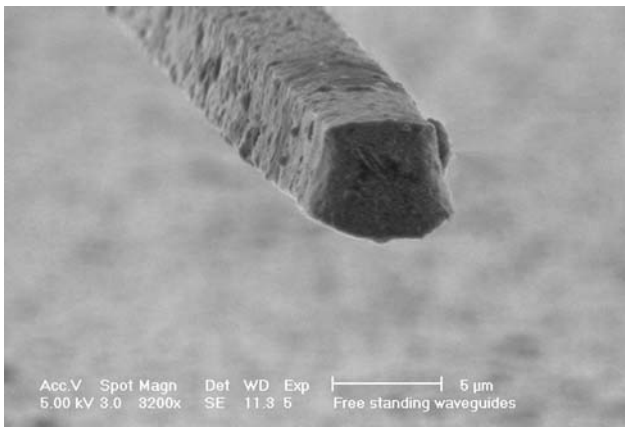

Fig. 1 Cross section of 0.5 MeV protons freestanding waveguide with air cladding

remained intact after removal of wax. This has encouraged us to investigate a possibility to improve the efficiency of the waveguides by reducing the pillar width. BeamPROP™ [15] has been used to study this effect in order to find a suitable pillar width, providing sufficient strength to hold the waveguide whilst causing a minimal loss. A channel waveguide with angled sidewalls has been used to approximate the waveguide structure, and three pillars have been embedded at 250, 500 and 750 μm in the *z*-direction. A modeled single mode fibre-field at the wavelength of 1.55 μm is launched into the waveguide. The intersection loss is plotted at each pillar, for a series of widths (Fig. 2). The simulation results show that, when the pillar width is reduced to a realizable value of 5 μm, there is less than 1% power loss at each intersection. A 10 mm long, freestanding waveguides can be fabricated with five supporting pillars, with a corresponding total intersection loss of only 0.3 dB. Figure 3 shows the cross-link of the freestanding waveguide with 5 μm wide supporting pillar.

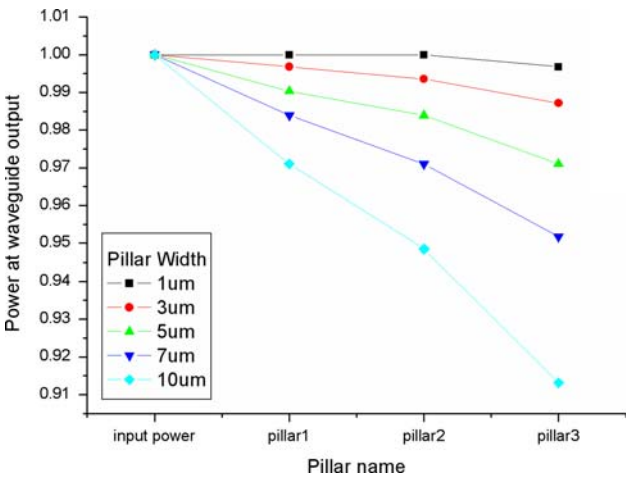

Fig. 2 Freestanding waveguide intersection loss induced by different pillar dimensions

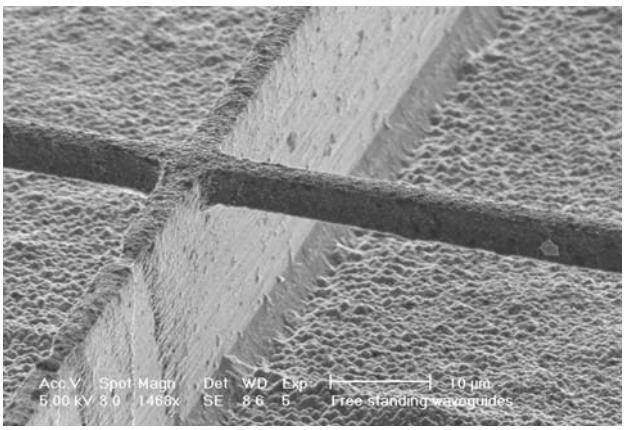

Fig. 3 Cross link of the freestanding waveguide with a supporting pillar. The waveguide and pillar are implanted with 0.5 and 2 MeV protons respectively

The measured losses of 13–14 dB/cm are mainly due to high energy proton induced defects and interface roughness. Annealing at 1,130 °C for 1/2 h is efficient to control migration of interstitials and concentration of the defects comparable to the state before the irradiation [16]. Because of high index difference ($\Delta n = 2.4$), the scattering loss is also important. In order to analyse the roughness, atomic force microscopy (AFM) has been implemented in this case. The average value of the roughness for different samples was 50 nm, while the correlation length was calculated to be 300 nm. The loss is simulated using BeamPROP^{TM}, and the propagation loss estimated to 5 dB/cm. Currently, we are investigating the use of thermal oxidation process to smooth out the waveguide roughness [17]. Annealing can be also used to anneal out the defects caused by proton irradiation in silicon. In our recent publication [18] we have shown that an annealing at 500 °C for 2 h can reduce the propagation loss of a different structure fabricated by the PBW from 20 to ~7 dB/cm. According to studies by Day and Horne [19] temperatures of 400–450 °C are sufficient to anneal out more than 90% of the defects, and therefore the remaining loss is mainly caused by the surface roughness. If we apply this conclusion to the freestanding waveguide, we can expect that the surface roughness contributes to the propagation loss by ~5 dB/cm, which is close to the prediction obtained by BeamPROP and AFM measurements. It is expected that this loss can be reduced to ~1 dB/cm after thermal oxidation [20].

3 Hollow-core waveguides for mid-wave infrared spectrum

As their name implies, hollow-core waveguides feature an air-filled core surrounded by walls made of multilayer coatings, designed to confine the propagating optical signal within the core. Since the light propagates through air in such waveguides, there is virtually no dispersion nor problems with temperature dependence of refractive index. The hollow-core waveguides can be also very useful for sensing applications as their core can be filled with gases or liquids. Other potential applications of these waveguides include tight turning radii and high power transmission. These waveguides can be classified in two categories: those with a Bragg-mirror cladding (e.g. [21]) and those with an ARROW (anti-resonant reflecting optical waveguide) cladding (e.g. [7]). The Bragg-mirror cladding comprises alternating layers of two types of materials, the so called "bilayers". In this case, light is totally reflected at the multilayer, for any incident angle or polarisation (hence the term "omnidirectional"), and therefore an optical mode can propagate in a low refractive index core. The multilayer cladding of ARROW waveguides is designed to behave like a Fabry-Perot interferometric reflector. The number of layers in this case can vary from only 1 to N.

Hollow core waveguides can be either on-chip or obtained by wafer bonding. In the former case, bottom cladding, core and top cladding are deposited on the same wafer, and then the core selectively etched, whilst in the latter case, a trench on one wafer is etched and a cladding deposited and then bonded to a second wafer where the other cladding has been deposited.

In this paper, we chose to analyze hollow-core omnidirectional waveguides (HOWs) with the Bragg-mirror cladding, optimized for MWIR spectrum. Recently, we have shown that HOWs with the Bragg mirror cladding based on silicon (Si) and silicon dioxide (SiO_2) multilayers are generally suitable for MWIR spectra [6]. It was shown that, due to a large difference in the refractive indices of Si and SiO_2, small propagation losses can be achieved with the waveguides having no more than five bilayers in the cladding. Also, the significance of the air-filled core size on the propagation losses was demonstrated.

In this paper, we further analyze the significance of core dimensions and number of bilayers in waveguides with the Bragg mirror cladding made of Si and SiO_2 bilayers. Specifically, we chose Si/SiO_2-based HOWs with the square core cross-section, as shown in Fig. 4a. Such waveguides are comprised of the upper and the lower sections made of two silicon wafers with deposited Bragg-mirror layers that form the hollow core in the middle. We have used a 3-D beam propagation method to calculate propagation losses in the waveguides for several different values of the core dimensions and overall number of bilayers in the cladding. All simulations were carried out for the He–Ne laser wavelength of $\lambda = 3.39$ µm. For the sake of better comparison, core dimensions (width and height) were expressed as multiples of the wavelength.

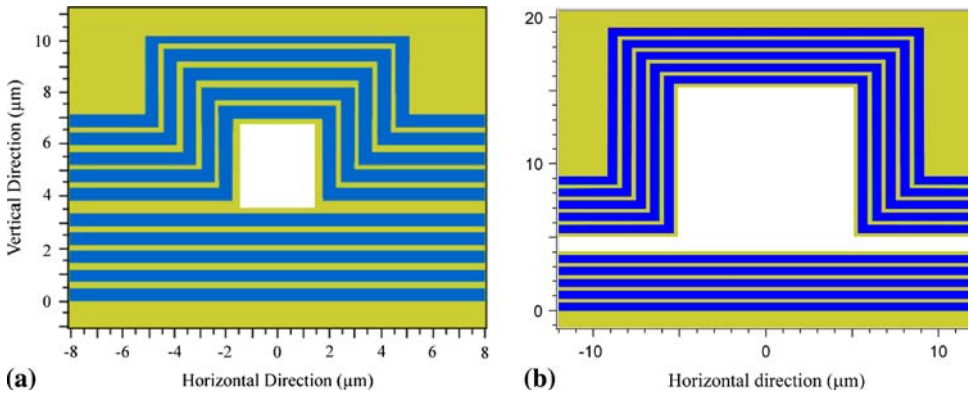

Fig. 4 (**a**) Hollow-core waveguide with a square cross-section (core size is arbitrary); (**b**) Hollow-core waveguide with an air gap between the lower and the upper claddings

Table 1 Propagation losses calculated for hollow-core waveguides with claddings based on Si/SiO_2 bilayers, at an emitting wavelength of He–Ne laser, $\lambda = 3.39$ μm

Core dimensions (width × height) (in wavelengths)	Number of bilayers in cladding	Propagation loss (dB/cm)
$2\lambda \times 2\lambda$	4	4.78
$2\lambda \times 2\lambda$	5	2.41
$3\lambda \times 3\lambda$	4	0.66
$3\lambda \times 3\lambda$	5	0.17
$3\lambda \times 3\lambda$ (air gap 1 μm)	5	0.44
$3\lambda \times 3\lambda$ (air gap 1.5 μm)	5	0.99
$4\lambda \times 4\lambda$	4	0.06

Calculated propagation losses for several waveguide structures are presented in Table 1.

These results show that waveguides with only four or five bilayers in the cladding, yet relatively large core dimensions of no less than three wavelengths in both width and height could exhibit propagation losses less than 1 dB/cm. Specifically, it is obvious that core dimensions have even greater impact on propagation losses than the overall number of bilayers in the cladding. Even for the waveguides with only four bilayers in the cladding, propagation loss (expressed in dB/cm) is reduced almost 10 times by increasing core size from $3\lambda \times 3\lambda$, to $4\lambda \times 4\lambda$.

These analyses were carried out for the ideal geometrical properties of the proposed square-shaped, hollow-core waveguides with a Si/SiO_2 Bragg-mirror cladding. Having in mind the fabrication procedure for such devices, this specific geometrical shape of the waveguide is difficult to produce. The process of fabrication would include making a trench in a silicon substrate, depositing alternating layers of SiO_2 and Si and than back-bonding another wafer with the deposited Bragg-mirror layers to eventually form a hollow-core waveguide with the square cross-section, as shown in Fig. 4a. However, due to such fabrication techniques, it is reasonable to expect that these two bonded wafers would not ideally fit to each other, and that an air-filled gap may be formed at the interface. This gap would result in a waveguide cross section shown in Fig. 4b.

In our further analysis, we have again used a 3-D beam propagation method to calculate propagation losses in the waveguides with such an air gap. Specifically, we chose the waveguide with five bilayers in the cladding and the core dimensions of $3\lambda \times 3\lambda$, where the wavelength was once again 3.39 μm. Previous analysis showed that this waveguide, without an air gap, exhibits relatively small propagation loss (Table 1). This time, our model included an air gap, resulting in a waveguide with the cross-section as shown in Fig. 4b. We have calculated the propagation loss for waveguides with 1 μm and 1.5 μm thick air gaps. Results are also presented in Table 1. It can be seen that a 1 μm thick gap increases the propagation loss to 0.44 dB/cm. For a larger gap of 1.5 μm, the loss is $\sim$1 dB/cm.

4 Conclusion

Freestanding waveguides were fabricated by PBW, and the cross sectional dimensions improved compared to our previous work. The waveguides had a 5.5 × 5.5 μm square like profile. The intersection loss with the supporting pillars was simulated for different dimensions of the pillars and for the pillar thickness of 5 μm that loss is expected to be 0.3 dB. The roughness of freestanding waveguides was analysed using AFM and BeamPROP^{TM} and its contribution to the propagation loss is within the expected values. Post fabrication treatment like thermal oxidation will help to smooth out the roughness and high temperature treatment will anneal out the defects caused by the proton irradiation.

Regarding the HOWs with a Si/SiO_2 Bragg-mirror cladding, we can say that they offer promising characteristics for the MWIR spectral range, especially in the wavelength range of 2.9–3.6 μm. The core size is an essential parameter and it is suggested that its both horizontal and vertical dimensions should be at least three times the wavelength for which the waveguide is designed.

Generally, the larger the core size, the lower the propagation loss. Reasonably small propagation losses can be achieved with only five or even four Si/SiO_2 bilayers, for such core dimensions. The presence of an air gap between the lower and upper sections of such waveguides can increase the propagation losses for the gaps with thickness of the order of 1 μm and more. In our future work, the effect of the air gap will be studied more comprehensively. Furthermore, a more realistic waveguide core geometry with slanted sidewalls (which is unavoidable in real devices due to the nature of the fabrication process) will be modelled. Also, the impact of surface roughness and layer thickness variations needs to be included in the analysis to provide more complete theoretical predictions.

References

1. A. Liu, R. Jones, L. Liao, D. Samara-Rubio, D. Rubin, O. Cohen, R. Nicolaescu, M. Panciccia, Nature **427**, 615 (2004)
2. H. Rong, R. Jones, A. Liu, O. Cohen, D. Hak, A. Fang, M. Paniccia, Nature **433**, 725 (2005)
3. V.R. Almeida, C.A. Barrios, R.R. Panepucci, M. Lipson, Nature **431**, 1081 (2004)
4. R.A. Soref, S.J. Emelett, W.R. Buchwald, J. Opt. A Pure Appl. Opt. **8**, 840 (2006)
5. P.Y. Yang, G.Z. Mashanovich, I. Gomez-Morilla, W.R. Headley, G.T. Reed, E.J. Teo, D.J. Blackwood, M.B.H. Breese, A.A. Bettiol, Appl. Phys. Lett. **90**, 241109 (2007)
6. S. Stanković, J. Crnjanski, G. Mashanovich, *Proceeding 51th Conference ETRAN* (Herceg-Novi, Montenegro, 2007), p. 49
7. R. Bernini, S. Campopiano, L. Zeni, IEEE J. Sel. Top. Quantum Electron. **8**, 106 (2002)
8. D. Yin, H. Schmidt, J.P. Barber, A.R. Hawkins, Opt. Express **12**, 2710 (2004)
9. H. Schmidt, D. Yin, J.P. Barber, A.R. Hawkins, IEEE J. Sel. Top. Quantum Electron. **11**, 519 (2005)
10. S.S. Lou, M.S. Wang, C.C. Chen, Opt. Express **12**, 6589 (2004)
11. J.F. Ziegler, J.P. Biersack, U. Littmark, in *The Stopping and Range of Ions in Solids* (Pergamon Press, New York, 1985)
12. P. Hovington, Scanning **19**, 29 (1997)
13. E.J. Teo, M.B.H. Breese, E.P. Tavernier, A.A. Bettiol, F. Watt, M.H. Liu, D.J. Blackwood, Appl. Phys. Lett. **84**, 3202 (2004)
14. M.B.H Breese, D. Mangaiyarkarasi, E.J. Teo, A.A. Bettiol, D. Blackwood, AIP Conf. Proc. **866**, 269 (2006)
15. Rsoft Design Group, Inc., 200 Executive Group Blvd. Ossining, NY 10562. (2002) http://www.rsoftdesign.com
16. S. Dannefaer, P. Mascher, D. Kerr, J. Appl. Phys. **15**, 3470 (1992)
17. K.K. Lee, D.R. Lim, L.C. Kimerling, Opt. Lett **26**, 1888 (2001)
18. E.J. Teo, A.A. Bettiol, M.B.H. Breese, P.Y. Yang, G.Z. Mashanovich, W.R. Headley, G.T. Reed, D.J. Blackwood, Opt. Express (submitted)
19. A.C. Day, W.E. Horne, I. Arimura, IEEE Trans. Nucl. Sci. **27**, 1665 (1980)
20. L. Lai, E.A. Irene, J. Appl. Phys. **86**, 1729 (1999)
21. G. Mashanovich, G. Pucker, C. Kompocholis, A. Lui, J. Crnjanski, S. Stankovic, V.M.N. Passaro, P. Matavulj, G.T. Reed, *Proceedings of 14th Telecom. Forum TELFOR 2006*, 3–6 November 2006, Belgrade, Serbia, pp. 357–360